Heliyon 10 (2024) e35663

Contents lists available at ScienceDirect

Heliyon

journal homepage: www.cell.com/heliyon

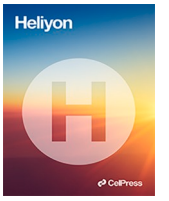

Research article

MicroRNA-2861 regulates the proliferation and apoptosis of human retinal vascular endothelial cells treated with high glucose by targeting NDUFB7

Qiqin Shi [a], Qiangsheng Wang [b], Ke Mao [c], Zhuoran Liu [a], Ruobing Wang [c,*]

[a] Department of Ophthalmology, Ningbo Hangzhou Bay Hospital, Ningbo, Zhejiang, 315000, China
[b] Department of Hematology, Ningbo Hangzhou Bay Hospital, Ningbo, Zhejiang, 315000, China
[c] Department of Ophthalmology, Renji Hospital, School of Medicine, Shanghai Jiao Tong University, Shanghai, 200127, China

ARTICLE INFO

Keywords:
Diabetic retinopathy
microRNA-2861
Apoptosis
Hyperglycemia
NDUFB7

ABSTRACT

Objectives: Although anti-VEGF and retinal laser photocoagulation are two therapeutic modalities that have been used in the clinical treatment of diabetic retinopathy (DR), it is unknown how these modalities target vascular endothelial function in DR.

Methods: We first downloaded and analyzed the differential genes in two DR-related datasets, GSE60436 and GSE53257. The differential gene expression was then verified using RT-qPCR, and the most upregulated gene, NDUFB7, was selected for subsequent experiments. Subsequently, the role of NDUFB7 silencing and enforced expression on the proliferation and apoptosis of HRVECs was explored using CCK-8 assay, EDU proliferation assay and apoptotic TUNEL staining. In addition, the upstream potential miRNAs of NDUFB7 were predicted online using the Targetscan website. RT-qPCR, Western blotting (WB), and dual luciferase gene reporter assay were used to confirm the targeting connection between miR-2861 and NDUFB7. Finally, miR-2861 expression after high glucose (HG) treatment and its effect on proliferation and apoptosis of HRVECs under HG were investigated.

Results: In this study, we first downloaded and analyzed the differential genes in two DR-related datasets, GSE60436 and GSE53257. We found that TUFM, PRELID1, MRPL32, NDUFB7, MRPL4, MRPL40, HSD17B10 and SLC25A13 were upregulated in DR, and RT-qPCR showed that NDUFB7 was most upregulated. Subsequent CCK-8 assay, EDU proliferation assay and TUNEL staining showed that up-picked NDUFB7 promotes proliferation and inhibits apoptosis of HRVECs. In addition, the upstream potential miRNAs of NDUFB7 were predicted online using the Targetscan website. RT-qPCR, Western blotting (WB), and dual luciferase gene reporter assay confirmed the targeting connection between miR-2861 and NDUFB7. Finally, it was observed that miR-2861 can inhibit the proliferation and promote the apoptosis of HRVECs by targeting NDUFB7.

Conclusions: Our findings showed that upregulated NDUFB7 in DR promotes proliferation and inhibits apoptosis of HRVECs, and miR-2861 can rescue the pathogenic effect of NDUFB7 upregulation by targeting NDUFB7.

* Corresponding author.
E-mail address: adawrb@126.com (R. Wang).

https://doi.org/10.1016/j.heliyon.2024.e35663
Received 12 October 2023; Received in revised form 31 July 2024; Accepted 1 August 2024
Available online 5 August 2024

1. Introduction

Diabetic retinopathy (DR), a major chronic blinding complication of the diabetic eye, has become an essential public health safety worldwide [1,2]. As research has progressed, DR is a simple progressive microvascular disease and a multi-tissue disease in which retinal neurovascular units (neurons, glial cells, vascular endothelial cells, and pericytes) are damaged [3,4]. The main features are increased permeability, angiogenesis, and neurodegenerative changes [5,6]. Human retinal vascular endothelial cells (HRVECs) are the main component of the retinal microvasculature with significance in DR through biological behaviors such as proliferation, migration, and angiogenesis [7,8]. Clinical treatments that are often utilized, such anti-VEGF and retinal laser photocoagulation, have drawbacks and a high recurrence rate [9–11]. However, targeting vascular endothelial function was less reported. Therefore, there is an urgent need to study the mechanism of DR progression further and provide new effective treatment strategies for DR.

Since the Human Genome Project concluded and the post-genomic era commenced, non-coding RNAs (ncRNAs) have garnered significant attention across diverse study domains [11,12]. MicroRNAs (miRNAs), small ncRNAs, can target the 3′ untranslated regions (UTRs) of mRNAs to directly regulate the degradation and translation of mRNAs [13,14]. By regulating different cell proliferation, differentiation, apoptosis, and autophagy, miRNAs indirectly affect the organism's physiological and pathological functions [15,16]. Increasing evidence shows that miRNAs are related to DR [17,18]. In previous reports, it has been proposed that miRNAs play a role in DR via controlling HRVEC migration, angiogenesis, apoptosis, and proliferation [17,19]. These studies provide valuable targets for DR therapy.

This study screened potential gene targets for DR therapy using bioinformatics, and the NDUFB7 gene was identified through further animal experiments and gene function validation. The relationship between miR-2861 and NDUFB7 was predicted using Targetscan and validated by dual luciferase and WB. Cellular assays were used to explore whether miR-2861 with NDUFB7 could regulate the proliferation and apoptosis of HRVECs. This study aims to refine the underlying pathophysiological mechanisms of DR, and we hope that our small step forward can provide some new ideas for the clinical treatment of this disease.

2. Research methods

2.1. Bioinformatic analysis

The datasets GSE60436 and GSE53257 were obtained from the Gene Expression Omnibus (GEO) database (https://www.ncbi.nlm.nih.gov/geo/). GSE60436 comprises gene expression profiles of fibrovascular membranes associated with proliferative diabetic retinopathy. It consists of three active fibrovascular membranes (FVMs) characterized by neovascularization, three inactive FVMs without neovascularization, and three gene expression profiles from normal human retinas. Conversely, GSE53257 contains six gene expression profiles from tissues of patients with Diabetic Retinopathy, five profiles from tissues of patients with a history of Diabetes, and five profiles from normal control retinas. The overall gene expression profiles from these datasets were examined for subsequent analysis.

On these two datasets, differential expression analysis was carried out independently. Using alternate criteria based on the R program limma, differentially expressed genes (DEGs) were found. KEGG and GO enrichment studies were carried out subsequently, utilizing the DEGs found in the preceding phase as a basis. These analyses aimed to elucidate the key pathways and functional annotations associated with the differential gene expression, specifically focusing on their relevance to DR.

Following this, a systematic analysis was conducted using the DEGs from both datasets to identify consistently up-regulated or down-regulated genes that could be potentially associated with DR. To validate the findings of our analyses, further experiments were conducted, with a particular focus on the gene NDUFB7. This gene was selected as the primary target for subsequent analysis and experimental investigation. A correlation study was conducted to obtain a more profound comprehension of the functional relationships and exchanges involving NDUFB7 and its linked genes. To find possible interactions and functional links, the Protein-Protein Interaction (PPI) network was examined using the STRING database (https://string-db.org/).

2.2. Cell lines and cell transfection

HRVECs (No. AC340362) and HEK293T cells were bought from ATCC (Manassas, VA). HEK293T was cultured in a DMEM medium (Gibco, CA, USA) supplemented with 10 % fetal bovine serum and 1 % penicillin-streptomycin at 37 °C in a 5 % CO2 incubator. HRVECs were cultured in a medium containing 25 mmol/L D-glucose in high glucose (HG) culture. Negative control plasmid and NDUFB7 plasmid were purchased from SangoBio (Shanghai, China), and miR-2861 mimics and si-NDUFB7 were purchased from Genepharma (Shanghai, China). Transfection was completed using Lipofectamine 8000 (Beyotime, Suzhou, China) when the cell confluence reached 50 %.

2.3. Fluorescence in situ hybridization (FISH)

FISH probes to detect the level of NDUFB7 by Cyanine3 labeling were provided by GenePharma Technology (China). The sequence was 5′-cttcattgaacagtttgtatattggaaacttgcc-3′. Prior to experimentation, the specificity of the FISH probe was rigorously verified through sequence alignment analysis and in vitro testing. HRVECs were fixed with 4 % paraformaldehyde (PFA) (Biosharp) for 15 min to preserve cellular morphology and prevent RNA degradation. Fixed cells were then incubated with the FISH probe targeting NDUFB7 at a concentration of 100 nM overnight at 37 °C in a humidity-controlled chamber. This facilitated the hybridization of the probe with the

target RNA sequences within the cells. Following hybridization, cells were washed with 2 × SSC (saline-sodium citrate) buffer to remove any unbound or nonspecifically bound probes and reduce background fluorescence. Using a fluorescent microscope fitted with the proper filter sets for Cyanine3 detection, the FISH-labeled cells were photographed.

2.4. Real-time quantitative PCR (RT-qPCR)

TRIzol reagent (Invitrogen) was used to extract total RNA from the cells, and a NanoDrop 2000 spectrophotometer (Thermo Fisher Scientific, USA) was used to measure the amount of RNA extracted. The mRNA was reverse transcribed using the PrimeScript™ RT kit (Takara, Japan), and the obtained cDNA was then quantified using the SYBR Green PCR Mixing Kit (Takara, Japan) labeled RT-qPCR assay according to the instructions. RT-qPCR for mRNA was run as follows: pre-denaturation at 95 °C for 5 min, denaturation at 95 °C for 30 s, annealing at 55 °C for 30 s, and extension at 72 °C for 15 s, 30 recycles. The miRNA was reverse transcribed using a miRNA 1st Strand cDNA Synthesis Kit (Sangon, China), and the obtained cDNA was then quantified using the miRNA Fluorescence PCR Kit (Sangon, China) labeled RT-qPCR assay according to the instructions. RT-qPCR for miRNA was run as follows: pre-denaturation at 95 °C for 30 s, denaturation at 95 °C for 5 s, annealing and extension at 60 °C for 30 s, and 40 recycles. The expression of mRNA and miRNA was quantified by the $2^{-\Delta\Delta}$ CT method using GAPDH and U6 as the internal reference, respectively. All primers were provided by Sangon Biotech (China), and the primer sequences are shown in Table 1.

2.5. Western blotting (WB)

A protein extraction kit (Sangon Biotech) was used to extract all of the proteins from the cells. Using the BCA kit, the total protein concentration was determined following the removal of the total protein. Fifty micrograms of total protein were added to 10 % SDS-PAGE protein separation gel for electrophoresis, and the program was set to concentrate at 60 V for 30 min and separate at a constant voltage of 100 V for 60 min. The proteins were then transferred to PVDF membranes (Merck Millipore, USA) and blocked. The membranes were incubated with anti-NDUFB7 (1:1000, Proteintech, China) and anti-GAPDH (1:5000, Proteintech, China) overnight at 4 °C. Following multiple TBST washes of the membranes, the strips were incubated for 1 h with a secondary antibody (1:3000, WanleiBio, China). Finally, enhanced chemiluminescence (ECL, Millipore, USA) chromogenic substrate was performed, and the results were analyzed by Image J software, with GAPDH as a normalized endogenous control.

Table 1
Primer sequences.

Gene name	Primer sequence
GAPDH	F 5'- ATTGTCAGCAATGCATCCTG -3'
	R 5'- ATGGACTGTGGTCATGAGCC -3'
HSD17B10	F 5'- TGGCGGTAATAACCGGAGGA -3'
	R 5'- ACAGTTGACAGCTACATCCACA -3'
MRPL4	F 5'- CTGGGTCTCAAAGTGGCACTG -3'
	R 5'- AACAGCCGGGATCAAGTTGAA -3'
MRPL32	F 5'- GGAGCGACTGCTACGGAAG -3'
	R 5'- GATACTGTCCAAAAGGCTGGAA -3'
MRPL40	F 5'- TCCGTGCTGCGAAGTATCTC -3'
	R 5'-AGTCTCTCTAAGCTGCGTCT-3'
PRELID1	F 5'- CTTGACGGAAGACATAGTACACC -3'
	R 5'- ACATTGGCAGGAAATAGTCGC -3'
SLC25A13	F 5'- GTGGAACTTTTAAGTGGAGTGGT -3'
	R 5'- TTGATGAATTGTGGTCTGTCCAA -3'
TUFM	F 5'- GGGGCTAAGTTCAAGAAGTACG -3'
	R 5'- CACATGAGCCGCATTGATGG -3'
NLRP3	F 5'- GATCTTCGCTGCGATCAACAG-3'
	R 5'- CGTGCATTATCTGAACCCCAC-3'
lL1B	F 5'- ATGATGGCTTATTACAGTGGCAA-3'
	R 5'- GTCGGAGATTCGTAGCTGGA-3'
CASP1	F 5'- TTTCCGCAAGGTTCGATTTTCA-3'
	R 5'- GGCATCTGCGCTCTACCATC-3'
miR-2861	F 5'- CTCGCTTCGGCAGCACA -3'
	R 5'- AACGCTTCACGAATTTGCGT -3'
U6	F 5'- GGGGCCTGGCGGTGGGC -3'
	R 5'- GAACATGTCTGCGTATCTC -3'

Notes: NLRP3, NLR family, pyrin domain containing 3; MRPL40, mitochondrial ribosomal protein L40; MRPL32, mitochondrial ribosomal protein L32; MRPL4, mitochondrial ribosomal protein L4; HSD17B10, hydroxysteroid (17-beta) dehydrogenase 10; lL1B, interleukin 1 beta; TUFM Tu translation elongation factor, mitochondrial; SLC25A13, solute carrier family 25, member 13 (citrin); PRELlD1, PRELl domain containing 1; CASP1, caspase 1, apoptosis-related cysteine peptidase.

2.6. CCK8 assay

The CCK8 assay examined cell viability after treatment with NDUFB7 and miR-2861. The cells were plated into 96-well plates. After 48 h or 72 h of treatment, 10 % CCK8 solution was added and incubated for 1 h. Then, the absorbance was measured at OD450 nm with a microplate reader.

2.7. Luciferase reporter assay

The wild-type luciferase plasmid (PmirGLO-NDUFB7-WT), mutant luciferase plasmid (PmirGLO- NDUFB7-MUT), and luciferase empty vector plasmid (PmirGLO) were synthesized by Biotech Bioengineering (Shanghai, China). NC mimics, and miR-2861 mimics were co-transfected with NDUFB7 wild-type or mutant luciferase plasmids in HEK293T cells. After 24 h, luciferase activity was detected using a dual-luciferase reporter kit (Beyotime, Suzhou, China).

2.8. EDU proliferation assay

The proliferation of each group after transfection was detected using the EDU kitThe precise procedures were adding 1 mL of diluted EDU solution with culture media (medium: EDU solution = 1000:1), setting the mixture at 37 °C for 2 h, discarding the supernatant, and fixing each well for 30 min with 200 μL of 4 % PFA. As directed by the EDU kit, 2 mg/mL of glycine solution (Solarbio, G8200, CAS: 56-40-6) and Apollo staining solution (Guangzhou RiboBio, C10310-3) were applied to each well. The wells were stained with DAPI for 30 min and then observed and photographed with a fluorescent microscope (Olympus BX51). We utilized ImageJ software to calculate the proliferation rate by determining the ratio of EDU-labeled proliferating cells to the total number of cells within a defined unit area of the microscope field. Ten random fields of view were analyzed to ensure representative sampling and accurate quantification of proliferating cells. Subsequently, GraphPad Prism software was employed to compute the relative expression levels of proliferation markers. This involved analyzing the density of EDU staining in comparison to the controls, enabling the determination of relative expression levels.

2.9. Apoptosis TUNEL staining

The cells mentioned above were fixed with 4 % PFA, and a TUNEL apoptosis kit (Servicebio, G1504-100T) was used to identify apoptosis. The apoptotic cells showed green fluorescence when observed under a laser-scanning confocal microscope. ImageJ software was utilzeed to calculate the apoptosis rate by determining the ratio of apoptotic cells to total cells within a defined unit area of the microscope field. Specifically, 10 random fields of view were analyzed to ensure representative sampling and accurate quantification of apoptotic cells. We sued GraphPad Prism software to compute the relative expression levels of the apoptotic markers. This involved analyzing the density of staining for apoptotic markers in comparison to the controls, enabling the determination of relative expression levels.

2.10. Animal experiment

We performed the animal experiments at Ready.Bio Co., LTD. We procured 10 male nine-week-old db/db diabetic mice, and feeded them a high-sugar, high-fat diet for five weeks. We monitored their fasting blood glucose levels (> 16.7 mmol/L) to confirm the presence of diabetes in the mice. Subsequently, we euthanized mice with isoflurane (RWD Life Science, R510-22) to obtain retinal tissue. Hematoxylin and eosin (HE) staining revealed that the retinal tissue thickness had become thinner in six of the db/db diabetic mice. Furthermore, there was a reduction in the number of ganglion cells, and a slight thickening was observed in the basal layer. These six mice served as the DR group and the other four mice served as the control group. Then the expression of NDUFB7 was detected.

2.11. Statistical analysis

Three runs of each experiment were conducted. Each and every value was given as mean ± standard deviation. The normalcy test was run using the Kolmogorov-Smirnov method. Depending on whether the data were normal, the Student's t-test or the Wilcoxon rank sum test were used to examine differences between continuous variables. An ANOVA in one direction was used to compare several groups. Using either Pearson correlation analysis (normal distribution) or Spearman correlation analysis (non-normal distribution), correlation analysis was carried out. The statistical analyses were performed using IBM, Armonk, NY, USA's SPSS Statistics 22.0. P values less than 0.05 indicated statistical significance for the difference.

3. Results

3.1. Candidate genes associated with DR

Upon obtaining the expression matrix for the two datasets, we initially examined the overall gene expression to ensure its unbiased nature. Subsequently, Principal Component Analysis (PCA) was performed to assess the differences between groups within each dataset (Fig. 1A and B). Differential Expression Analysis was conducted by comparing the samples with DR, leading to the

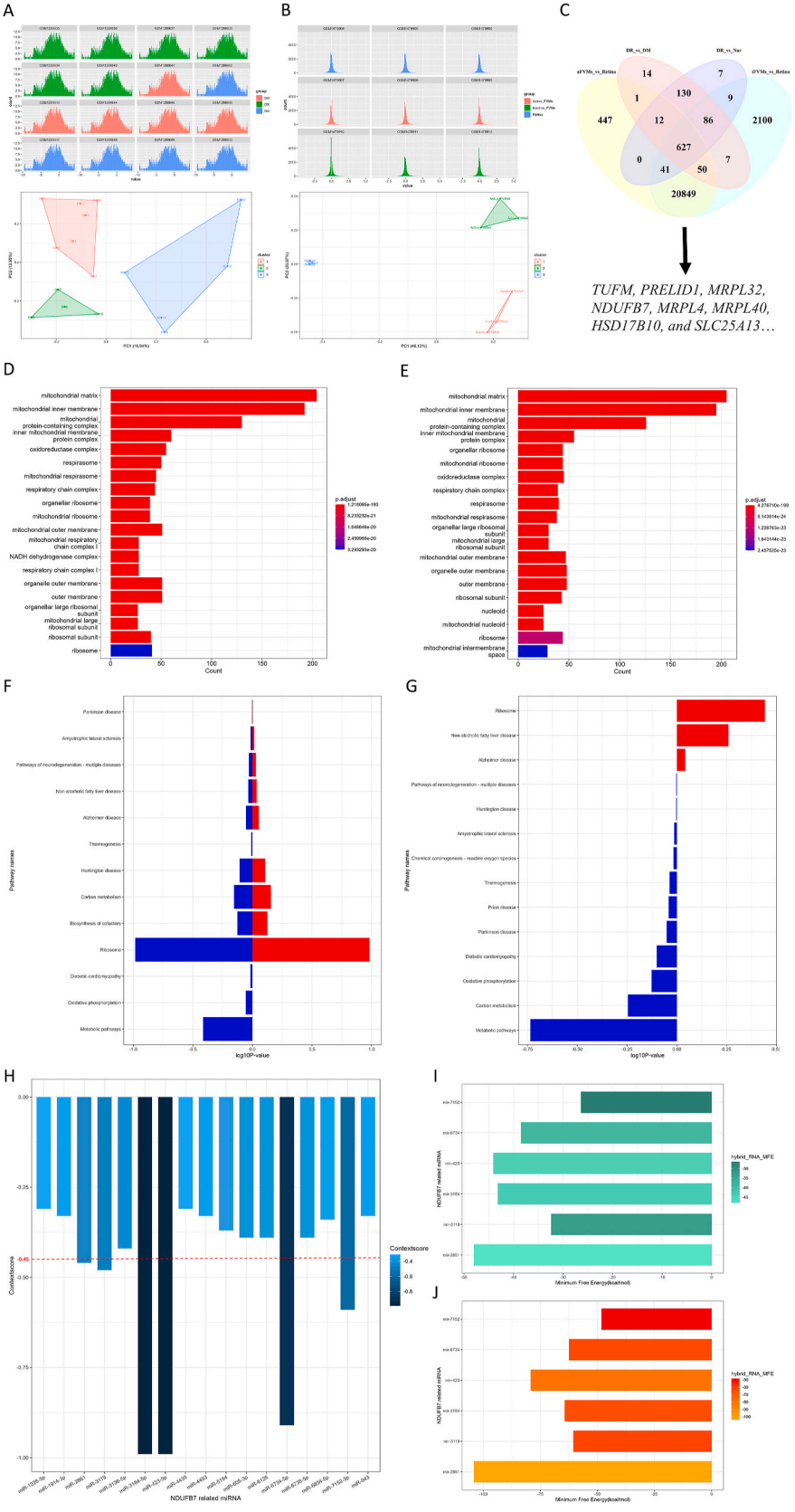

(caption on next page)

Fig. 1. Results of raw letter analysis against GSE60436 and GSE53257. A and B. Gene expression and PCA plot of GSE53257 and GSE60436. C. Vennplot of consistent DEGs within two datasets. D and E. GO enrichment analysis displays DEGs' significant enrichment in DR vs. Nor and DR vs. DM in GSE53257. F and G. GSEA KEGG enrichment analysis displaying the significant enrichment of DEGs in DR vs. Nor and DR vs. DM in GSE53257. H. ContextScore for miRNAs targeting NDUFB7, miRNAs with scores lower than −0.45 (the red dot line) were selected. **I-J.** RNAhybrid analysis demonstrating the miRNAs' MFE (kcal/mol) interact with 3′UTR and CDS region of NDUFB7.

identification of several DEGs in DR, including TUFM, PRELID1, MRPL32, NDUFB7, MRPL4, MRPL40, HSD17B10, and SLC25A13 (Fig. 1C).

GO enrichment was used to DR to gain insights into the functional implications of these DEGs. The results revealed significant enrichment of differential genes in GO terms associated with the mitochondrial matrix, mitochondrial transport, mitochondrial inner membrane, and mitochondrial complex (Fig. 1D and E). Furthermore, GSEA KEGG pathway enrichment analysis using the same grouping method highlighted the enrichment of DEGs in pathways related to the biosynthesis of cofactors and ribosomes (Fig. 1F and G). These findings strongly suggest a close association of these genes with the underlying disease mechanism.

3.2. Validation of candidate genes

To verify whether the screened genes were associated with DR abnormalities, we performed validation by cellular experiments. HRVECs were cultured in HG medium and subsequently subjected to RT-qPCR for candidate genes. The results are shown in Fig. 2A. NDUFB7 had the highest expression among all candidate genes. To further verify this conclusion, we detected the expression of NDUFB7 in the DR group and in the control group. NDUFB7 expression was found to be substantially greater in the DR group than in the control group (Fig. 2B and C, and Supplementary Fig. 1). Meanwhile, retinal HE and immunohistochemical staining also proved this conclusion (Fig. 2D and E). Among them, NDUFB7 belongs to NADH ubiquinone oxidoreductase subunit B7, and the expression of NDUFB7 and the diagnosis and treatment of DR-related diseases have not been reported.

In addition to the screening results of NDUFB7, we investigated the correlation between NDUFB7 and other up-regulated DEGs. In both GEO datasets, our research showed a significant connection between NDUFB7 and two other DEGs, TUFM and PRELID1 (Fig. 2F and G). Furthermore, the Protein-Protein Interaction (PPI) network demonstrated a strong correlation between NDUFB7 and products of other up-regulated genes (Fig. 2H). The positive correlations between NDUFB7, TUFM, PRELID1 and others suggest potential functional associations among these genes. The PPI Network analysis further supports the interconnectedness between NDUFB7 and other up-regulated genes at the protein level. Further investigations are warranted to elucidate these interrelationships' functional implications and underlying mechanisms.

3.3. Effect of NDUFB7 on the proliferation and apoptosis of HRVECs

To discuss whether DR is related to the expression of NDUFB7, we cultured HRVECs in HG (90 % HG DMEM + 10 % FB), HG + Si-NC (HG-treated cells transfected with Si-NC), HG + Si- NDUFB7 (HG-treated cells transfected with Si-NDUFB7), HG + vector (HG-treated cells transfected with null plasmid), HG + Vector-NDUFB7 (HG-treated cells transfected with NDUFB7 overexpression plasmid) media, respectively. RT-qPCR and WB assay experimental results are shown in Fig. 3A and B, and Supplementary Fig. 2. NDUFB7 expression was much higher in the HG + Vector- NDUFB7 group than it was in the other groups. Additionally, in HG + Si-NDUFB7, the expression of NDUFB7 was considerably lower than in the other groups. Next, we verified the correlation between cell proliferation and apoptosis in each group. Fig. 3C shows cell proliferation was highest in the HG + Vector-NDUFB7 group and lowest in the HG + Si-NDUFB7 group. These results indicate that NDUFB7 gene expression promoted the proliferation of HRVECs. The EDU studies showed that the NDUFB7 overexpression group had a considerably larger number of EDU-positive cells than the control group (Fig. 3D and **F**). The results of the TUNEL apoptosis staining assay are shown in Fig. 3E and **G**. Apoptotic cells were unicellular with dense, brown nuclei, and non-apoptotic cells had blue nuclei. The findings of the CCK8 and EDU tests were further supported by the fact that there was substantially less apoptosis in the HG + Vector-NDUFB7 group than in the HG + Si-NDUFB7 group.

3.4. Targeted regulation of NDUFB7 by miR-2861

The prediction results obtained from TargetScan indicated that miR-2861, miR-423-5p, miR-3184-5p, miR-6734-5p, and miR-5194 may regulate NDUFB7. To identify miRNAs with superior regulatory functions, we utilized ContextScore and selected those with lower scores, indicating stronger regulatory potential (Fig. 1H). To further evaluate the interaction between miRNAs and NDUFB7, we employed RNAhybrid to calculate the characteristics of the hybrid RNA formed between the miRNA and NDUFB7, considering both the coding sequence (CDS) region and the 3′UTR region. Among the results, miR-2861 exhibited the lowest Minimum Free Energy (MFE), indicating a more stable binding between the two RNA molecules and a higher likelihood of interaction (Fig. 1I and J).

The observed sequence and thermodynamic characteristics align with previous findings in the literature, where decreased expression of miR-2861 has been reported in the context of diabetic nephropathy [20]. Consequently, miR-2861 was selected as the upstream miRNA for subsequent investigations.

HRVECs were divided into miR-NC, miR-2861 mimics, and miR-2861 inhibitors to verify the targeting effect of miR-2861 and NDUFB7. RT-qPCR and WB showed that the expression of miR-2861 differed among the three groups, indicating that miR-2861 and NDUFB7 may have a targeting relationship (Fig. 4A and B, and Supplementary Fig. 3). The results of the dual luciferase reporter assay

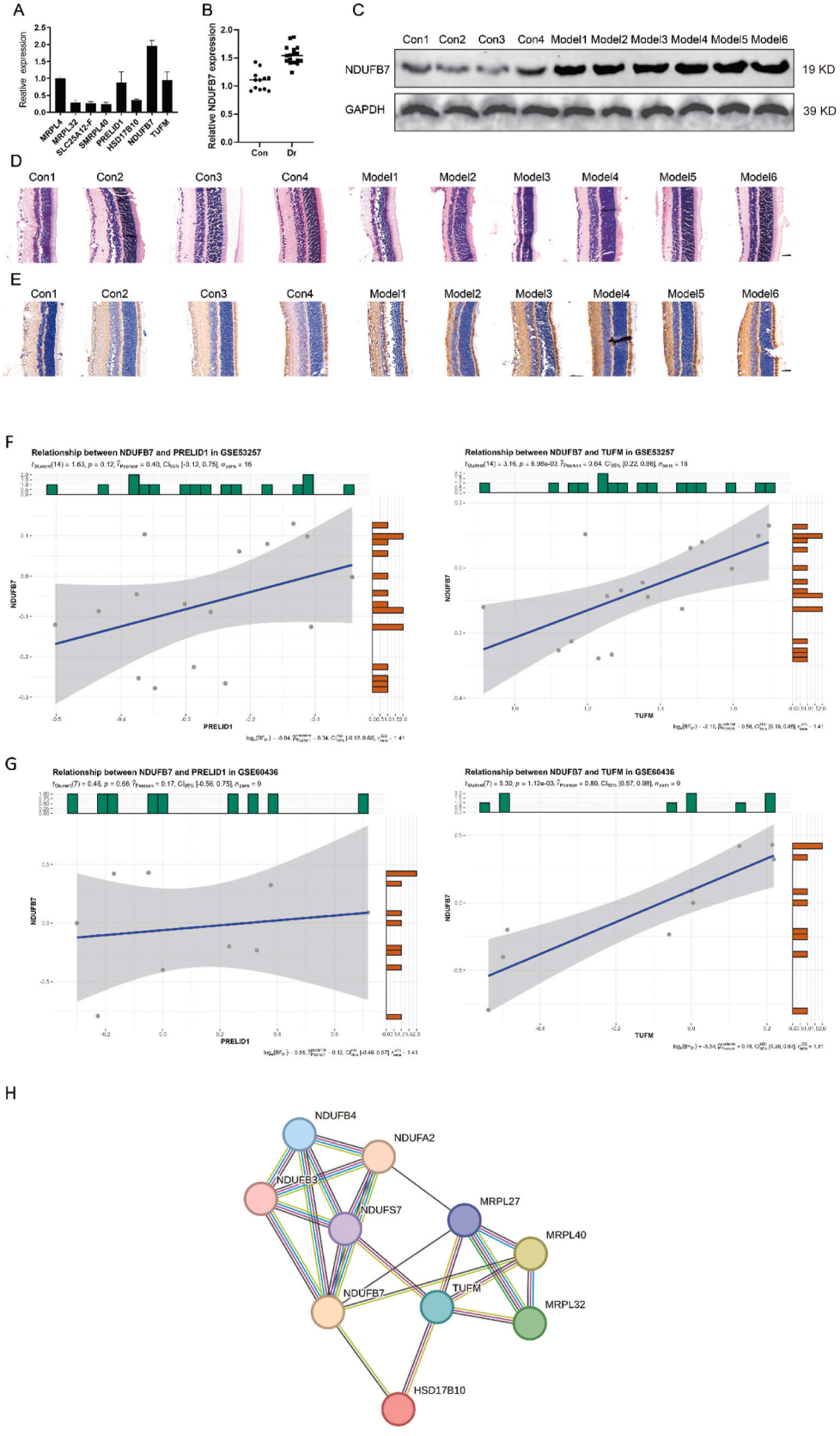

(caption on next page)

Fig. 2. In vivo and in vitro validation of common differential gene expression patterns. A. RT-qPCR was used to detect the relative expression of TUFM, PRELID1, MRPL32, NDUFB7, MRPL4, MRPL40, HSD17B10, and SLC25A13 mRNAs in HG medium. **B.** RT-qPCR was used to detect NDUFB7 mRNA expression in the retinas of normal mice (n = 4) and diabetic mice (n = 6) using RT-qPCR. **C.** WB was used to detect the protein expression of NDUFB7 in each group. **D.** Hematoxylin & eosin staining of the retinas of normal mice (n = 4) and diabetic mice (n = 6). Scale bar = 100 μm. **E.** Immunohistochemical staining was used to detect NDUFB7 protein expression in the retinas of normal mice (n = 4) and diabetic mice (n = 6). Scale bar = 100 μm. **F and G.** Correlation analysis illustrates the positive correlation between NDUFB7 and TUFM and PRELID1 in the two GEO datasets. **H.** Protein-Protein Interaction Network (PPI Network) highlighting the strong correlation between NDUFB7 and other up-regulated genes at the protein level.

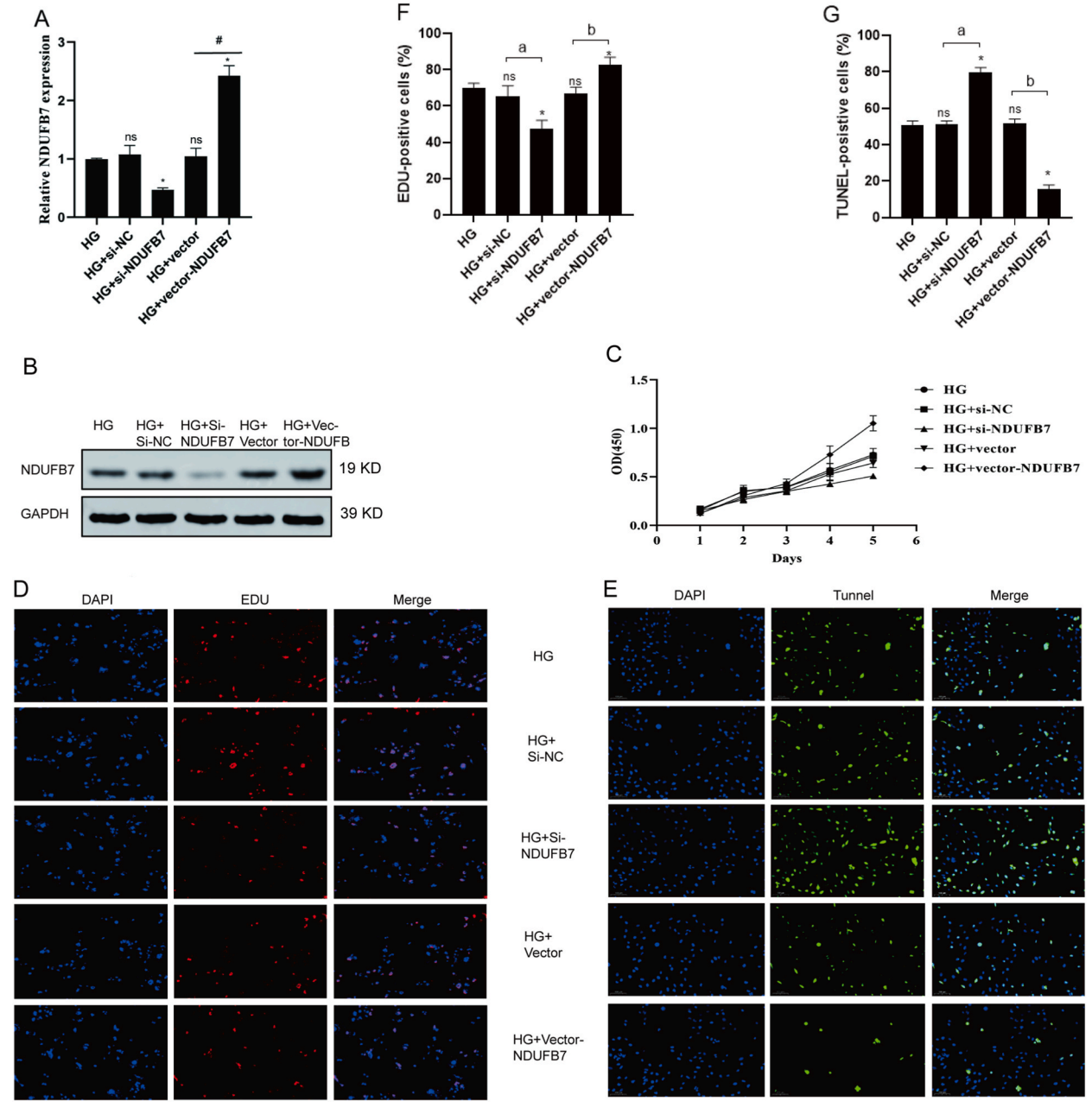

Fig. 3. Effect of NDUFB7 on proliferation and apoptosis of HG treated HRVECs. A-B. RT-qPCR **(A)** and Western Blotting **(B)** were used to detect the mRNA and protein expression of NDUFB7 in each group, respectively. **C.** CCK8 assay was used to detect cell viability in each group. **D-E.** EDU proliferation assay **(D)** and TUNEL staining **(E)** were used to detect proliferating and apoptotic cells in each group of cells. Scale bar = 100 μm. **F-G.** Quantitative analysis of EDU proliferation assay **(F)** and TUNEL staining **(G)**. HG: HG (90 % HG DMEM + 10 % FB); HG + Si-NC: HG-treated cells transfected with Si-NC; HG + Si- NDUFB7: HG-treated cells transfected with Si-NDUFB7 knockdown NDUFB7; HG + vector: HG-treated cells transfected with null plasmid; HG + Vector-NDUFB7: HG-treated cells transfected with NDUFB7 overexpression plasmid. *: $P < 0.05$, compared with HG group; a: $P < 0.05$, compared with HG + Si-NC group; b: $P < 0.05$ compared with HG + Vector group.

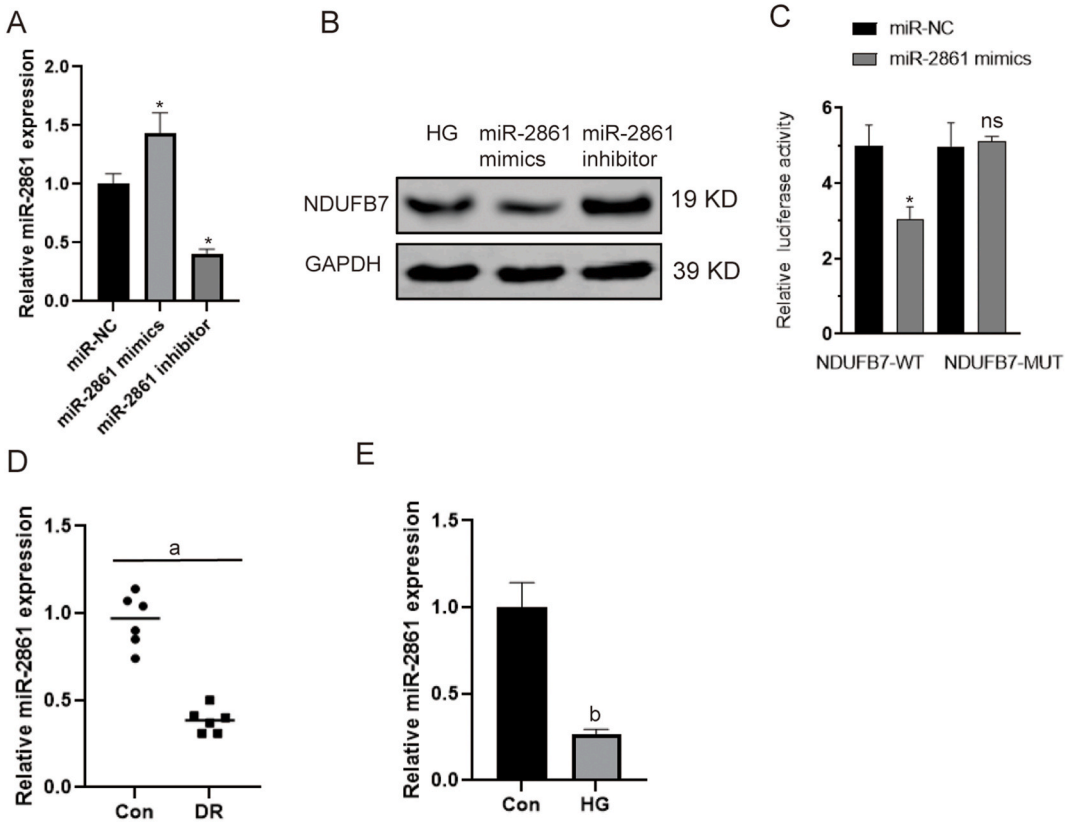

Fig. 4. NDUFB7 is the target gene of miR-2861. A. RT-qPCR was used to detect the expression of miR-2861 in each group. **B.** WB was used to detect the protein expression of NDUFB7 in each group. **C.** Dual luciferase reporter assay was used to verify the targeting relationship between NDUFB7 and miR-2861. **D.** RT-qPCR was used to detect miR-2861 expression in the retinas of normal mice (n = 4) and diabetic mice (n = 6). **E.** RT-qPCR was used to detect expression in HG-treated and normal cultured HRVECs. *: $p < 0.05$, compared with miR-NC group; ns: $p > 0.05$, compared with miR-NC group; a: $p < 0.05$, compared with control (con) group; b: $p < 0.05$, compared with control (con) group.

showed that, in contrast to the miR-NC group, miR-2861 dramatically reduced the luciferase of the NDUFB7 wild type, while the mutant type showed no discernible change (Fig. 4C). This result suggests that miR-2861 can target the expression of NDUFB7. The DR group's miR-2861 expression was considerably lower than that of the control group (Fig. 4D and **E**). These results further validated the targeting relationship between miR-2861 and NDUFB7.

3.5. Effect of miR-2861/NDUFB7 on the proliferation and apoptosis of HRVECs

To explore the effect of miR-2861/targeted regulation of NDUFB7 expression on the proliferation and apoptosis of HRVECs, we divided the cells into five groups: HG, HG + miR-NC, HG + miR-2861 mimics, HG + miR-2861 mimics + Vector, and HG + miR-2861 mimics + NDUFB7. RT-qPCR and WB revealed that NDUFB7 expression was reduced after adding miR-2861 mimics, indicating that miR-2861 can target and regulate NDUFB7 (Fig. 5A and B, and Supplementary Fig. 4). The results of the cell proliferation assay are shown in Fig. 5C. The addition of miR-2861 mimics significantly decreased cell proliferation and elevated apoptosis (Fig. 5D–5G). Compared with the HG + miR-2861 mimics + vector group, cell proliferation was increased and apoptosis was decreased in the HG + miR-2861 mimics + NDUFB7 group (Fig. 5D–G). These results indicated that miR-2861 can target and regulate NDUFB7 to regulate HRVECs function.

4. Discussion

Although many studies have explored the pathological mechanisms of DR, less can be used for clinical treatment. Consequently, understanding the molecular causes of DR and creating a novel treatment are clinically important [21,22]. There is growing evidence that vascular endothelial cell dysfunction stimulated by hyperglycemia underlies the pathology of DR [23,24]. Furthermore, through controlling a number of important variables that are represented by VEGF, including as cell proliferation, apoptosis, inflammatory response, microcirculatory damage, and oxidative stress, miRNAs control distinct pathogenic alterations throughout the onset and progression of DR [25,26]. As a result, a novel class of medications called miRNA antagonists or analogs may be able to stop or delay

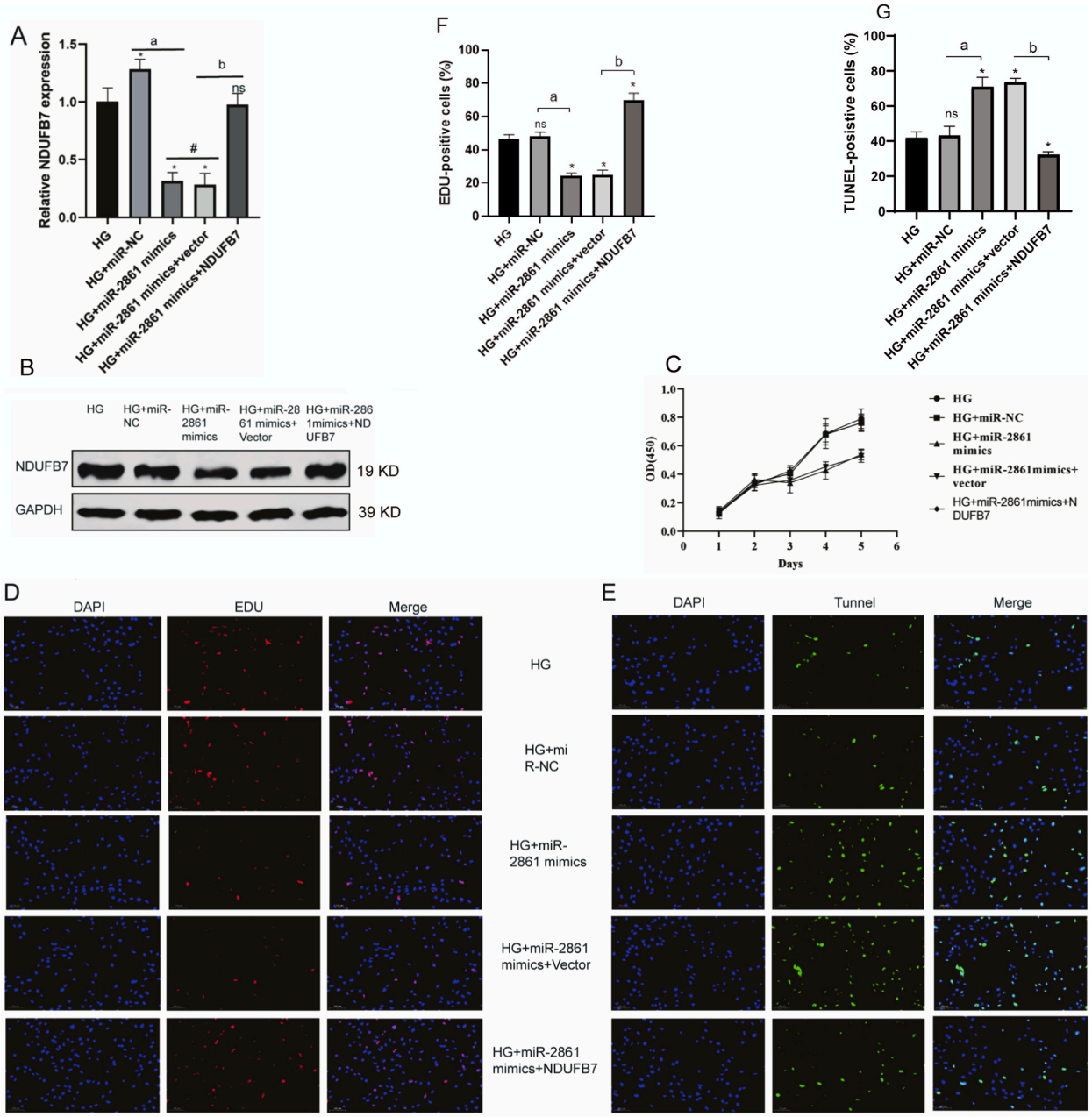

Fig. 5. Effect of miR-2861 on proliferation and apoptosis of HRVECs treated with HG. A-B. RT-qPCR **(A)** and Western Blotting **(B)** were used to detect the mRNA and protein expression of NDUFB7 in each group, respectively. **C.** CCK8 assay was used to detect cell viability in each group. **D-F.** EDU proliferation assay **(D)** and TUNEL staining **(F)** were used to detect proliferating and apoptotic cells in each group of cells. **F-G.** Quantitative analysis of EDU proliferation assay **(F)** and TUNEL staining **(G)**. Scale bar = 100 μm. HG: HG; HG + miR-NC: HG-treated cells transfected with miR-NC; HG + miR-2861 mimics: HG-treated cells transfected with miR-2861 mimics; HG + miR-2861 mimics + Vector: HG-treated cells transfected with miR-2861 mimics and null plasmid; HG + miR-2861 mimics + Vector-NDUFB7: HG-treated cells transfected with miR-2861 mimics and NDUFB7 overexpression plasmid. *: $P < 0.05$ compared with HG group; ns: $P > 0.05$, compared with HG group; a: $P < 0.05$, compared with HG + miR-NC group; #: $P < 0.05$ compared with HG + miR-2861 mimics group; b: $P < 0.05$, compared with HG + miR-2861 mimics + Vector-NDUFB7 group.

the development and spread of DR lesions.

In this paper, we identified several potential target genes associated with DR by bioinformatic analysis of a database of mRNAs closely related to DR expression, among which NDUFB7 belongs to the NADH ubiquinone oxidoreductase subunit B7. In previous studies, NDUFB7 was associated with depression, Parkinson's disease, psoriatic arthritis, severe congenital lactic acidosis, and hypertrophic cardiomyopathy [27–29]. It is the first study to report NDUFB7 expression and DR correlation. Ellis et al. demonstrated

endothelial cells' role in ROS production in the early stages of retinopathy in BBZ/Wor rats, an obese, non-insulin-dependent model of diabetes [30]. Oxidative stress and inflammatory responses are the fundamental pathogenic mechanisms involved in DR. The hexosamine pathway, polyol pathway, late glycation end products/receptors, and protein kinase C activation are all increased by hyperglycemia and lead to oxidative stress, reactive oxygen species (ROS) buildup, and apoptosis, all of which promote pro-inflammatory responses [31–33]. Producing mediators and chemokines induce retinal neurodegenerative changes, disrupting the blood-retinal barrier, increasing vascular permeability and neovascularization, and exacerbating DR neurovascular dysfunction [34,35]. Additionally, we showed through cellular and animal tests that NDUFB7 expression was considerably up-regulated in the DR group. Next, we verified the function of the NDUFB7 gene. The experimental results showed that NDUFB7 could promote the proliferation of HRVECs.

This study also revealed that miR-2861 could target the regulation of NDUFB7 expression in diabetic retinopathy. MiR-2861 was closely related to osteogenic differentiation and tumors [36–38]. The most important human investigation to find miRNA biomarkers for DN and LN generated from histological biopsies linked to renal associations of pathological lesions and functional indicators of kidney damage was provided by Mariana et al. [39]. In DN patients, miR-2861 was related to SCr and eGFR in the BKBx and UW cohorts [40]. Furthermore, in the histopathological assessment of BKBx, miR-2861 was related to interstitial fibrosis, tubular atrophy (IFTA), as well as tubulointerstitial inflammation in areas of fibrosis [39]. Furthermore, the present study not only found the downregulation of miR-2861 in HRVECs after high-glucose treatment but also showed that it was significantly downregulated in a mouse model of DR. Therefore, miR-2861 may be helpful as a biomarker for DR. In future work, we can further investigate the function of miR-2861 as a biomarker of DR and demonstrate the therapeutic significance of miR-2861 in vivo experiments.

This study has several limitations. One limitation of this study is the focus on in vitro and animal model experiments, which may not fully capture the complexity of DR as it manifests in humans. While these models provide valuable insights into cellular mechanisms and potential therapeutic targets, the translation of findings from bench to bedside requires further validation in clinical settings. Furthermore, the study's main focus was on determining how miR-2861 and NDUFB7 affected HRVEC proliferation and apoptosis in HG environments. However, DR is a multifactorial disease involving various cell types, molecular pathways, and environmental factors. Thus, the contribution of other miRNAs, target genes, and signaling pathways to the pathogenesis of DR cannot be overlooked. Future studies should investigate the interactions between various miRNAs and their targets in order to have a more thorough understanding of the pathophysiology of DR.

5. Conclusion

Up-regulated NDUFB7 in DR promoted the proliferation and inhibited the apoptosis of HRVECs. MiR-2861 can rescue the pathogenic effects of NDUFB7 upregulation by targeting NDUFB7. miR-2861/NDUFB7 axis has the potential to be an effective strategy for DR treatment and deserves further promotion.

Data availability statement

The data associated with this study has not been deposited into a publicly available repository. Data will be made available on request.

Funding statement

This work was supported by the National Natural Science Foundation of China (81770932 and 82171061), the Natural Science Foundation of Shanghai (22ZR1438400) and the Natural Science Foundation of Ningbo (2022J053).

Ethics statement

The studies involving animal experiments were reviewed and approved by the Animal Ethics Committee of the Renji Hospital of Shanghai Jiaotong University School of Medicine (RJ2022-0930) and conducted according to the declaration of Helsinki.

CRediT authorship contribution statement

Qiqin Shi: Writing – original draft, Visualization, Validation, Supervision, Software, Resources, Project administration, Methodology, Investigation, Funding acquisition, Formal analysis, Data curation, Conceptualization. **Qiangsheng Wang:** Writing – original draft, Investigation, Data curation, Conceptualization. **Ke Mao:** Writing – review & editing, Software, Methodology. **Zhuoran Liu:** Validation, Software, Resources, Investigation, Formal analysis. **Ruobing Wang:** Writing – review & editing, Writing – original draft, Visualization, Resources, Project administration, Investigation, Funding acquisition.

Declaration of competing interest

The authors declare that they have no known competing financial interests or personal relationships that could have appeared to influence the work reported in this paper.

Appendix A. Supplementary data

Supplementary data to this article can be found online at https://doi.org/10.1016/j.heliyon.2024.e35663.

References

[1] X. Zhao, F. Ling, G.W. Zhang, N. Yu, J. Yang, X.Y. Xin, The correlation between MicroRNAs and diabetic retinopathy, Front. Immunol. 13 (2022) 941982.
[2] D. Zheng, N. Li, R. Hou, X. Zhang, L. Wu, J. Sundquist, K. Sundquist, J. Ji, Glucagon-like peptide-1 receptor agonists and diabetic retinopathy: nationwide cohort and Mendelian randomization studies, BMC Med. 21 (2023) 40.
[3] Y.-X. Xu, S.-D. Pu, X. Li, Z.-W. Yu, Y.-T. Zhang, X.-W. Tong, Y.-Y. Shan, X.-Y. Gao, Exosomal ncRNAs: novel therapeutic target and biomarker for diabetic complications, Pharmacol. Res. 178 (2022) 106135.
[4] C. Meng, C. Gu, S. He, T. Su, T. Lhamo, D. Draga, Q. Qiu, Pyroptosis in the retinal neurovascular unit: new insights into diabetic retinopathy, Front. Immunol. 12 (2021) 763092.
[5] Y. Yang, Y. Liu, Y. Li, Z. Chen, Y. Xiong, T. Zhou, W. Tao, F. Xu, H. Yang, S. Ylä-Herttuala, S.S. Chaurasia, W.-C. Adam, K. Yang, MicroRNA-15b targets VEGF and inhibits angiogenesis in proliferative diabetic retinopathy, J. Clin. Endocrinol. Metab. 105 (2020).
[6] J.B. Cole, J.C. Florez, Genetics of diabetes mellitus and diabetes complications, Nat. Rev. Nephrol. 16 (2020) 377–390.
[7] Q. Wang, X. Zhang, K. Wang, L. Zhu, B. Qiu, X. Chen, X. Lin, Y. Nie, An model of diabetic retinal vascular endothelial dysfunction and neuroretinal degeneration, J. Diabetes Res. 2021 (2021) 9765119.
[8] T. Zhang, H. Ouyang, X. Mei, B. Lu, Z. Yu, K. Chen, Z. Wang, L. Ji, Erianin alleviates diabetic retinopathy by reducing retinal inflammation initiated by microglial cells via inhibiting hyperglycemia-mediated ERK1/2-NF-κB signaling pathway, FASEB J 33 (2019) 11776–11790.
[9] M.L. Rodríguez, S. Pérez, S. Mena-Mollá, M.C. Desco, Á.L. Ortega, Oxidative stress and microvascular alterations in diabetic retinopathy: future therapies, Oxid. Med. Cell. Longev. 2019 (2019) 4940825.
[10] E.B. Parente, V. Harjutsalo, C. Forsblom, P.-H. Groop, Waist-height ratio and the risk of severe diabetic eye disease in type 1 diabetes: a 15-year cohort study, J. Clin. Endocrinol. Metab. 107 (2022) e653–e662.
[11] J. Friedrich, D.H.W. Steel, R.O. Schlingemann, M.J. Koss, H.-P. Hammes, G. Krenning, I. Klaassen, microRNA expression profile in the vitreous of proliferative diabetic retinopathy patients and differences from patients treated with anti-VEGF therapy, Transl Vis Sci Technol 9 (2020) 16.
[12] S. Hombach, M. Kretz, Non-coding RNAs: classification, biology and functioning, Adv. Exp. Med. Biol. 937 (2016).
[13] S. Wang, A. Talukder, M. Cha, X. Li, H. Hu, Computational annotation of miRNA transcription start sites, Briefings Bioinf. 22 (2021) 380–392.
[14] B. Bouzari, S. Mohammadi, D.O. Bokov, I.I. Krasnyuk, S.R. Hosseini-Fard, M. Hajibaba, R. Mirzaei, S. Karampoor, Angioregulatory role of miRNAs and exosomal miRNAs in glioblastoma pathogenesis, Biomed. Pharmacother. 148 (2022) 112760.
[15] D. Sengupta, M. Deb, S. Kar, N. Pradhan, S. Parbin, R. Kirtana, S.P. Singh, S.G. Suma, Niharika, A. Roy, S. Manna, P. Saha, P. Chakraborty, S. Dash, C. Kausar, S. K. Patra, Dissecting miRNA facilitated physiology and function in human breast cancer for therapeutic intervention, Semin. Cancer Biol. 72 (2021) 46–64.
[16] L. Chen, L. Heikkinen, C. Wang, Y. Yang, H. Sun, G. Wong, Trends in the development of miRNA bioinformatics tools, Briefings Bioinf. 20 (2019) 1836–1852.
[17] S. Zhao, H. Wang, H. Xu, Y. Tan, C. Zhang, Q. Zeng, L. Liu, S. Qu, Targeting the microRNAs in exosome: a potential therapeutic strategy for alleviation of diabetes-related cardiovascular complication, Pharmacol. Res. 173 (2021) 105868.
[18] F. Barutta, B. Corbetta, S. Bellini, S. Guarrera, G. Matullo, M. Scandella, C. Schalkwijk, C.D. Stehouwer, N. Chaturvedi, S.S. Soedamah-Muthu, M. Durazzo, G. Gruden, MicroRNA 146a is associated with diabetic complications in type 1 diabetic patients from the EURODIAB PCS, J. Transl. Med. 19 (2021) 475.
[19] Y. Liu, Q. Yang, H. Fu, J. Wang, S. Yuan, X. Li, P. Xie, Z. Hu, Q. Liu, Müller glia-derived exosomal miR-9-3p promotes angiogenesis by restricting sphingosine-1-phosphate receptor S1P in diabetic retinopathy, Mol. Ther. Nucleic Acids 27 (2022) 491–504.
[20] M. Cardenas-Gonzalez, A. Srivastava, M. Pavkovic, V. Bijol, H.G. Rennke, I.E. Stillman, X. Zhang, S. Parikh, B.H. Rovin, M. Afkarian, Identification, confirmation, and replication of novel urinary microRNA biomarkers in lupus nephritis and diabetic nephropathy, Clin. Chem. 63 (2017) 1515–1526.
[21] Q. Kang, C. Yang, Oxidative stress and diabetic retinopathy: molecular mechanisms, pathogenetic role and therapeutic implications, Redox Biol. 37 (2020) 101799.
[22] H.-P. Hammes, Diabetic retinopathy: hyperglycaemia, oxidative stress and beyond, Diabetologia 61 (2018) 29–38.
[23] D. Tonade, T.S. Kern, Photoreceptor cells and RPE contribute to the development of diabetic retinopathy, Prog. Retin. Eye Res. 83 (2021) 100919.
[24] S.-L. Zhu, M.-L. Wang, Y.-T. He, S.-W. Guo, T.-T. Li, W.-J. Peng, D. Luo, Capsaicin ameliorates intermittent high glucose-mediated endothelial senescence via the TRPV1/SIRT1 pathway, Phytomedicine 100 (2022) 154081.
[25] P. Kaur, S. Kotru, S. Singh, A. Munshi, miRNA signatures in diabetic retinopathy and nephropathy: delineating underlying mechanisms, J. Physiol. Biochem. 78 (2022) 19–37.
[26] Z. Zhang, C. Song, T. Wang, L. Sun, L. Qin, J. Ju, miR-139-5p promotes neovascularization in diabetic retinopathy by regulating the phosphatase and tensin homolog, Arch Pharm. Res. (Seoul) 44 (2021) 205–218.
[27] Y. Wang, Y. Liu, Z. Jin, C. Liu, X. Yu, K. Chen, D. Meng, A. Liu, B. Fang, Association between mitochondrial function and rehabilitation of Parkinson's disease: revealed by exosomal mRNA and lncRNA expression profiles, Front. Aging Neurosci. 14 (2022) 909622.
[28] S.P. Correia, M.F. Moedas, K. Naess, H. Bruhn, C. Maffezzini, J. Calvo-Garrido, N. Lesko, R. Wibom, F.A. Schober, A. Jemt, H. Stranneheim, C. Freyer, A. Wedell, A. Wredenberg, Severe congenital lactic acidosis and hypertrophic cardiomyopathy caused by an intronic variant in NDUFB7, Hum. Mutat. 42 (2021) 378–384.
[29] K. Henningsen, J. Palmfeldt, S. Christiansen, I. Baiges, S. Bak, O.N. Jensen, N. Gregersen, O. Wiborg, Candidate hippocampal biomarkers of susceptibility and resilience to stress in a rat model of depression, Mol. Cell. Proteomics 11 (2012) 016428. M111.
[30] E.A. Ellis, D.L. Guberski, B. Hutson, M.B. Grant, Time course of NADH oxidase, inducible nitric oxide synthase and peroxynitrite in diabetic retinopathy in the BBZ/WOR rat, Nitric Oxide 6 (2002) 295–304.
[31] H. Rao, J.A. Jalali, T.P. Johnston, P. Koulen, Emerging roles of dyslipidemia and hyperglycemia in diabetic retinopathy: molecular mechanisms and clinical perspectives, Front. Endocrinol. 12 (2021) 620045.
[32] Y. Tu, L. Li, L. Zhu, Y. Guo, S. Du, Y. Zhang, Z. Wang, Y. Zhang, M. Zhu, Geniposide attenuates hyperglycemia-induced oxidative stress and inflammation by activating the Nrf2 signaling pathway in experimental diabetic retinopathy, Oxid. Med. Cell. Longev. 2021 (2021) 9247947.
[33] S.-B. Catrina, X. Zheng, Hypoxia and hypoxia-inducible factors in diabetes and its complications, Diabetologia 64 (2021) 709–716.
[34] U.M. Kinuthia, A. Wolf, T. Langmann, Microglia and inflammatory responses in diabetic retinopathy, Front. Immunol. 11 (2020) 564077.
[35] A. Sheemar, D. Soni, B. Takkar, S. Basu, P. Venkatesh, Inflammatory mediators in diabetic retinopathy: deriving clinicopathological correlations for potential targeted therapy, Indian J. Ophthalmol. 69 (2021) 3035–3049.
[36] W. Bu, X. Xu, Z. Wang, N. Jin, L. Liu, J. Liu, S. Zhu, K. Zhang, R. Jelinek, D. Zhou, H. Sun, B. Yang, Ascorbic acid-PEI carbon dots with osteogenic effects as miR-2861 carriers to effectively enhance bone regeneration, ACS Appl. Mater. Interfaces 12 (2020) 50287–50302.
[37] J. Xu, X. Wan, X. Chen, Y. Fang, X. Cheng, X. Xie, W. Lu, miR-2861 acts as a tumor suppressor via targeting EGFR/AKT2/CCND1 pathway in cervical cancer induced by human papillomavirus virus 16 E6, Sci. Rep. 6 (2016) 28968.

[38] X.-P. Zhou, Q.-W. Li, Z.-Z. Shu, Y. Liu, TP53-mediated miR-2861 promotes osteogenic differentiation of BMSCs by targeting Smad7, Mol. Cell. Biochem. 477 (2022) 283–293.
[39] M. Cardenas-Gonzalez, A. Srivastava, M. Pavkovic, V. Bijol, H.G. Rennke, I.E. Stillman, X. Zhang, S. Parikh, B.H. Rovin, M. Afkarian, I.H. de Boer, J. Himmelfarb, S.S. Waikar, V.S. Vaidya, Identification, confirmation, and replication of novel urinary MicroRNA biomarkers in lupus nephritis and diabetic nephropathy, Clin. Chem. 63 (2017) 1515–1526.
[40] D. Delić, C. Eisele, R. Schmid, P. Baum, F. Wiech, M. Gerl, H. Zimdahl, S.S. Pullen, R. Urquhart, Urinary exosomal miRNA signature in type II diabetic nephropathy patients, PLoS One 11 (2016) e0150154.